

Automatic Identification of Critical Damage Value with In-situ Shearing Test and Notched Plate Tensile Test with Image Analysis

Yoshinori Yoshida^{1*} and Asuka Kutsukake²

¹Gifu University, Centre for Advanced Die Engineering and Technology (G-CADET), 1-1 Yanagi-do, Gifu 501-1193, Japan

²Shimane University, Next Generation Tatara Co-Creation Centre (NEXTA), 1060 Nishikawatsu-cho, Matsue 690-8504, Japan

Abstract. Critical damage values in Cockcroft and Latham's and Ayada's models are automatically identified using autonomous-driven finite element analysis (ADFEA). To validate fracture behavior, we perform in-situ shearing and tensile tests on notched steel plates, employing image analysis. In ADFEA, a machine-learning-based optimization algorithm searches for critical damage values by minimizing the error between simulated and experimental fracture test results. The dependence of critical damage value identification on the testing method is demonstrated, and the effectiveness of fracture prediction theories and material testing methods for finite element analysis of shear processing is discussed.

Keywords: Ductile fracture; Shearing test; Notched plate tensile test; Autonomous-driven FEA

1 Introduction

The critical damage value for integral-type ductile fracture is typically identified through fracture testing, often using tensile tests. However, tensile tests result in fracture after at most a few tens of percent elongation, whereas the shearing process can introduce strains exceeding 100% before fracture. The difference in stress triaxiality history raises questions about the validity of critical damage values obtained from tensile tests for large-strain processes such as the shearing process. This study applied inverse analysis with machine learning-based optimization in finite element analysis (FEA) to determine the critical damage value through shearing process simulations. The results were compared with values from tensile tests using image analysis to assess the influence of strain history.

2 Experimental methods

2.1 In-situ shearing test

Shearing experiments were performed on 0.2 mm-thick low-carbon cold-rolled steel SPCC (JIS) sheets using a specialized die designed for in-situ observation of sheet metal shearing. A schematic diagram of the experiment is presented in Fig. 1 (left). The shearing process was recorded with a high-speed camera through a side window in the die. The experimental conditions are depicted also in Fig. 1 (right). Each experiment was conducted three times under identical conditions, and

the sheared surface length was measured at five points across the specimen width.

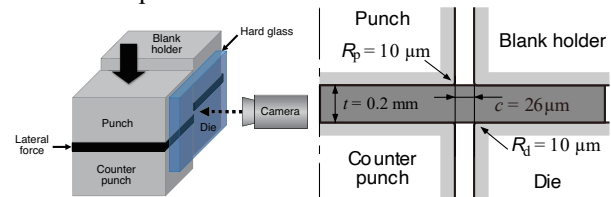


Fig. 1. Schematic diagram of the in-situ observation system for plane-strain shearing and its experimental conditions.

2.2 Notched tensile test with image analysis

To experimentally measure the necking shape, tensile tests were conducted on notched plate specimens. Fig. 2 (left) shows the test specimens used. The necking width w , necking curvature radius R , and necking thickness t were continuously recorded from the start of the test to final fracture using two charge-coupled device (CCD) cameras (Fig. 2 (right)). The captured images were converted to monochrome for analysis.

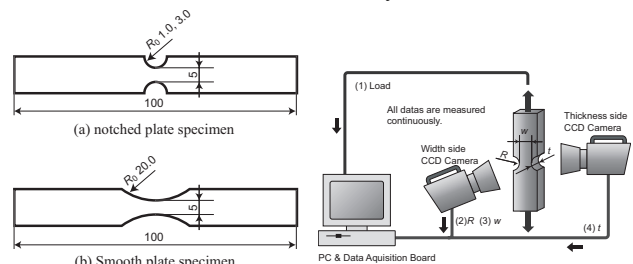


Fig 2. Notched tensile test specimens and testing method.

* Corresponding author: yoshida.yoshinori.p9@f.gifu-u.ac.jp

The width-side images were used to determine necking width and curvature radius, while the thickness-side images were analyzed to measure necking thickness. Normal strains at the necking are expressed as follows,

$$\varepsilon_w = \ln \frac{w}{w_0}, \quad \varepsilon_t = \ln \frac{t}{t_0} \quad \varepsilon_w = -(\varepsilon_w + \varepsilon_t) \quad (1)$$

Equivalent strain $\bar{\varepsilon}$ was calculated by the normal strains defined by equation (1). Analysis of various stress components in necking was carried out by Bridgman's correction [1]. They are calculated by the following equations. Here, it is assumed that stress field is uniaxial, and material flow is isotropic at the necking,

$$\begin{cases} \sigma_{max} = \sigma_{za} \left[1 + \ln \left(1 + \frac{w}{4R} \right) \right] \\ \frac{\sigma_m}{\bar{\sigma}} = \frac{1}{3} + \ln \left(1 + \frac{w}{4R} \right) \end{cases} \quad (2)$$

where σ_m is average of normal stresses, σ_{za} is tensile axial stress components which is defined as follows,

$$\begin{cases} \sigma_{za} = \frac{\sigma_{zav}}{\sqrt{1 + 4 \frac{R_w}{w} \ln \left[1 + \frac{w}{2R_w} + \left(\frac{w}{R_w} \right)^{1/2} \left(1 + \frac{1}{4} \frac{w}{R_w} \right)^{1/2} \right] - 1}} \\ \sigma_{zav} = \frac{P}{wt} \end{cases} \quad (3)$$

where P is the tensile load and σ_{zav} is the average tensile stress in the necking cross-section.

As an integral-type ductile fracture criterion, Cockcroft & Latham (C&L) model[2] was applied with following equation,

$$C_f = \int^{\bar{\varepsilon}_f} \sigma_{max} d\bar{\varepsilon} \quad (4)$$

where σ_{max} and C_f are maximum principal stress and critical damage value. C_f was identified by the notched plate tensile test with image analysis and inverse FEA of the shearing process experiment.

3 Analysis Method

Finite element analysis (FEA) of SPCC sheet shearing was performed using the general-purpose software DEFORM™ 2D. The sheet thickness was set to 0.2 mm, consistent with the experimental conditions. The specimen was modeled as an elasto-plastic body, while the die was treated as a rigid body. A 2D plane-strain model was assumed. The specimen was meshed with 8,000 elements, and Coulomb's friction law was applied with a friction coefficient of $\mu = 0.2$. The tool settings matched those used in the experiment.

Fig. 3 illustrates the workflow for critical damage value identification using autonomous-driven FEA (ADFEA) based on a surrogate-based optimization (SBO) algorithm. As described earlier, the C&L model was applied as the fracture criterion, and the sheared surface length was used as the objective variable. The absolute difference between the experimental and simulated values was defined as the error E [mm], expressed as follows:

$$E = |SSL_{FEA} - SSL_{exp}| \quad (5)$$

where SSL_{FEA} and SSL_{exp} represent the simulated and measured sheared surface lengths, respectively.

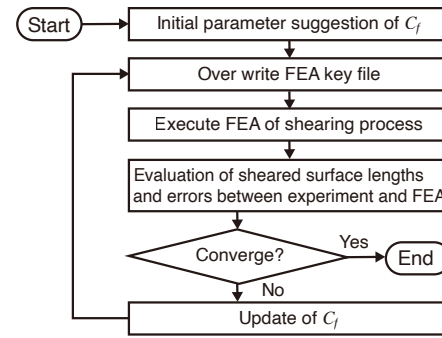


Fig. 3 Workflow for critical damage value identification using ADFEA based on the SBO algorithm.

The critical damage value C_f was automatically identified to minimize E . The search range for C_f was set

$$\begin{cases} \sigma_{za} = \frac{\sigma_{zav}}{\left\{ 1 + 4 \frac{R_w}{w} \ln \left[1 + \frac{w}{2R_w} + \left(\frac{w}{R_w} \right)^{1/2} \left(1 + \frac{1}{4} \frac{w}{R_w} \right)^{1/2} \right] - 1 \right\}^{1/2}} \text{ Pa.} \\ \sigma_{zav} = \frac{P}{wt} \end{cases}$$

As a result of ADFEA, the optimal critical damage value was determined to be 2070 MPa. On the other hand, the critical damage values obtained from notched tensile tests of sheet specimens using image analysis and stress correction based on Bridgman's method are shown in Table 1. As the initial notch radius increased, the critical damage value also increased; however, the maximum value was 938 MPa, which is less than half of the 2070 MPa obtained through inverse analysis in this study.

Table 1. Critical damage values obtained from the notched tensile test.

Initial notch radius [mm]	Critical damage value [MPa]
1.0	702.9
3.0	800.2
20.0	938.0

4 Conclusions

By integrating an optimization method based on machine learning with shearing process experiments and finite element analysis, the critical damage value in the Cockcroft & Latham model was automatically identified. The results revealed a discrepancy between the critical damage value obtained from tensile tests using image analysis and the identified value. Future research will focus on refining fracture condition equations and improving methods for determining critical damage values under large deformation conditions.

References

1. P.W. Bridgman, *Studies in large plastic flow and fracture*, 9 (McGraw-Hill, 1952).
2. M.G. Cockcroft and D.J. Latham, *J. Inst. Met.*, **96**, 33 (1968).